



## DEVELOPMENT OF AN INSTALLATION TO REDUCE THE TEMPERATURE OF PHOTOVOLTAIC MODULES AND IMPROVE THEIR EFFICIENCY

R. Mazón-Hernández, JR García-Cascales, F Vera-García, A Sánchez-Kaiser, B Zamora-Parra  
Thermal and Fluid Engineering Department, Technical University of Cartagena, Doctor Fleming, s/n  
30202, Cartagena, Murcia, Spain

Email: [rmh@alu.upct.es](mailto:rmh@alu.upct.es), [jr.garcia@upct.es](mailto:jr.garcia@upct.es), [francisco.vera@upct.es](mailto:francisco.vera@upct.es), [antonio.kaiser@upct.es](mailto:antonio.kaiser@upct.es),  
[blas.zamora@upct.es](mailto:blas.zamora@upct.es)

**Abstract.** The main priority in photovoltaic panels is electricity production. The transformation of solar energy into electricity depends on the operating temperature in such a way that the lower the temperature is, the better the performance of the panels is. In the existing literature, different cooling techniques may be found. Most of them propose the use of air or water as thermal energy carriers. This paper is focused on the use of these cooling techniques in photovoltaic panels placed onto the roof of a greenhouse. So, the objective of this study is to ensure a low operating temperature which corrects and reverses the effects produced by high temperature on efficiency.

### Keywords

Efficiency improvement, temperature decrease, experimental facilities, temperature influence, solar panels

### 1. Introduction

Photovoltaic cells allow the direct conversion of solar energy into electrical energy with maximum efficiency at around 9-12%, depending on the type of solar cells. More than 80% of the solar radiation reaching the photovoltaic cell (PV) is not converted into electricity; it is reflected or transformed into heat energy.

The heat generated yields to an increase in cell temperature and consequently to a decrease in conversion efficiency of electricity. According to Angrist et al. [1-3], this inverse relationship of output power (conversion efficiency) with temperature is mainly due to the dependence of the open circuit voltage,  $V_{oc}$  with temperature.

The negative effect of the temperature increase on the performance of the panel is an important factor to consider. Special concern deserves new applications such as those based on using photovoltaic energy produced by the panels in greenhouses. In this application, the photovoltaic

panels are located onto the roof of the greenhouse, with an air duct between the two surfaces. In this study, we analyse the effect of the temperature on the performance for different sections, varying the thickness of the duct.

The use of air as thermal energy carrier to cool photovoltaic panels can be done by using either a "chimney effect" provoked by natural convection or forced convection through a driving duct form at the rear surface of the panel as Tiwari et al. suggest in [4].

In this work, a facility developed to study different geometries of ducts is presented. An uncertainty analysis of the different variables measured and calculated is included. Experimental results obtained for different cross section are shown. Due to the paper extension limitation only the results obtained for constant cross sections and natural convection are included in this paper. Some conclusions and a brief description of the studies still ongoing are finally drawn.

### 2. Experimental facility

The solar installation consists of two photovoltaic panels arranged as shown in Figure 1. A first panel (panel A) is used as reference panel. Panel temperature at different points, voltage, and current are measured to understand the panel behaviour under normal operating conditions and to compare with another one (panel B) which is modified to test different ducts with different cross sections.

In this second panel, surface temperature at different points, voltage, and current are also measured jointly with the air temperature and air flow rate. Figure 2 shows schematically the photovoltaic panel cooled by natural convection, with all the instrumentation required for data collection and their subsequent analyses. In the solar panels, temperatures are measured with RTD, and wind speed with hot film anemometers.



Fig. 1. Solar panels. Left panel (A), right panel (B).

The horizontal components of solar radiation are measured by two pyranometers. Other environmental conditions such as temperature, atmospheric pressure, humidity, and wind speed are measured with a meteorological station placed on our laboratory roof just beside the experimental facility. All data are registered and recorded by means of a data logger.

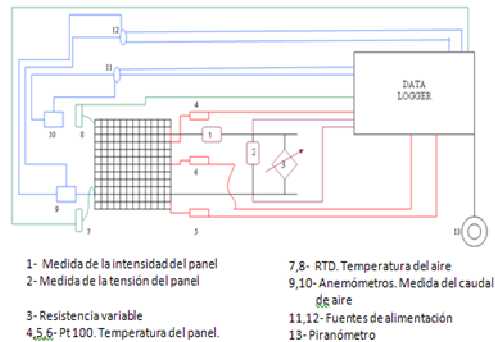


Fig. 2 Diagram of solar system

### 3. Description of the instrumentation used

In this section shows the main features of the sensors used with greater emphasis on accuracy or class B uncertainty to make an analysis of the uncertainty in the data collection.

Table 1 gives the description of the sensors mentioned above:

Sensor	Characteristics	Accuracy
Flexible and robust Pt100 Probe	- Measure the temperature of the panel – Range:-50°C a 150°C	Quality B ±0.3°C
Precision Pt100 probe	- Measure the temperature of the air flow -Range:-50°C 250°C	Quality A ±0.15°C
Hot film anemometer	- Measure the air velocity, natural convection Range:0-2m/s	±0.06m/s
Hot film anemometer	-Measure the air velocity, forced convection Range:0-20m/s	±0.2m/s
Precision	- Measure the global	

pyranometer	radiation -Range:0 – 1200W/m <sup>2</sup>	±9μV/W m <sup>2</sup>
Current transducers	-Measure the current -Range:	<±1%
Voltage transducers	-Measure the voltage -Range:	±0.9%
Variable load	- Electronic governor - Get the curve I-V - Range: 0-100 V 0-10 A	±1mV ±5mA

Table 1. Sensor description.

### 4. Analysis of the data uncertainty

The uncertainty is defined as "a parameter associated with the result of a measure that characterises the range of values that can be reasonably attributed to the measure". Uncertainty and error are interrelated and that uncertainty should consider all possible sources of error of the measurement process.

The uncertainty concept reflects doubts about the veracity of the result once all possible sources of error. Therefore, it gives an idea of the quality of the result and shows the range within which the estimated value is considered true. They have been evaluated and the necessary corrections have been applied. The procedure followed in their evaluation is described in what follows.

In general, the result of a measure can be expressed by a magnitude  $x$  as:  $x = \mu \pm u_i$  where  $\mu$  is the value measured and  $u_i$  is the uncertainty which includes the scale error, systematic error, and accidental or random error.

To calculate the uncertainty of all measurable variables, two types of uncertainty are considered, class A and class B. The class A uncertainty is obtained by statistical methods from values. The class B is the uncertainty of each sensor as mentioned in the preceding paragraph that is,  $U_{class B} = \text{Sensor accuracy}$  on Table 1. The total uncertainty of each measure is then given by:  $U^2 = \sqrt{U_{class A}^2 + U_{class B}^2}$

To calculate the uncertainty of class A, let us assume "n" measures of a magnitude ( $x_i$ ) obtained in the same conditions and using the same method. Assuming that errors are distributed according to a Gaussian distribution, the value of the magnitude will coincide with its mean,  $\mu$ . The measurement uncertainty will be related to its standard deviation,  $\sigma$ , which is a measure of data dispersion around the mean.

Usually the mean and standard deviation are not known but can be from the data, so

$$\bar{x} = \frac{\sum_{i=1}^n x_i}{n} \quad s = \sqrt{\frac{\sum_{i=1}^n (x_i - \bar{x})^2}{n-1}}$$

Thus, the uncertainty of the panel temperature, air temperature, wind speed, voltage and current of the panel can be calculated by:

$$U_{classA} = s = \sqrt{\frac{\sum_{i=1}^n (x_i - \bar{x})^2}{n-1}}$$

However, the irradiance, power, and performance cannot be measured, because they are calculated from measured variables, therefore their uncertainty are calculated differently.

When one wants to calculate the uncertainty of a variable which cannot be measured, but is obtained from other measurable variables the combined uncertainty should be calculated. It is carried out by applying the "uncertainty propagation law".

The relationship between measured variables and the variable to be calculated is given by:  $Y = f(X_1, X_2, X_3, \dots)$ . If variables  $X_1, X_2, X_3, \dots$  are independent, which is true in this case, then these variables are uncorrelated; and the uncertainty of  $Y$  is given by:

$$U_c(Y) = \sqrt{\sum_{i=1}^n \left(\frac{\partial f}{\partial X_i}\right)^2 \cdot U^2(X_i)}$$

However, if the measured variables are correlated, the uncertainty of  $Y$  is obtained:  $U_c(Y) =$

$$\sqrt{\sum_{i=1}^n \left(\frac{\partial f}{\partial X_i}\right)^2 U^2(X_i) + 2 \sum_{i=1}^{n-1} \sum_{j=i+1}^n \left(\frac{\partial f}{\partial X_i}\right) \left(\frac{\partial f}{\partial X_j}\right) U(X_i) U(X_j) r(X_i, X_j)}$$

where  $r(X_i, X_j)$  is the regression coefficient [5].

The uncertainty propagation law is applied to obtain the uncertainty of the irradiance, power, and performance. The relationships they have with the measured variables are:

$$I_{rr} = \frac{P_{m}}{S_{panel}} \quad \left\{ \begin{array}{l} I_{rr} = \text{Irradiance (W)} \\ I_{pira} = \text{Pyranometer measure (W/m}^2\text{)} \\ S_{panel} = \text{Panel area (m}^2\text{)} \end{array} \right.$$

$$P_m = I_{mp} \cdot V_{mp} \quad \left\{ \begin{array}{l} P_m = \text{Maximum power (W)} \\ I_{mp} = \text{Current (m.p.) (A)} \\ V_{mp} = \text{Voltage (m.p.) (V)} \end{array} \right.$$

$$\eta = \frac{P_m}{I_{rr} \cdot S_{panel}} = \frac{I_{mp} \cdot V_{mp}}{I_{rr} \cdot S_{panel}} \quad \eta = \text{Panel performance}$$

#### 4.1. Uncertainty of the experimental results

To calculate the uncertainty of the variables measured in the experiments, 25 samples of measurable variables have been collected the same day and under the same environmental conditions.

The uncertainties obtained are very good, which means that the data collected are sufficiently reliable. The results are presented in Table 2 and 3.

PANEL A				
Variable	Mean	Uncert. Class A	Uncert. Class B	Uncertainty
T <sub>panel,1</sub>	46.9636	0.6309	0.300	<b>0.6987 °C</b>
T <sub>panel,2</sub>	40.8158	0.9123	0.300	<b>0.9603 °C</b>
T <sub>panel,3</sub>	51.9077	0.5171	0.300	<b>0.5979 °C</b>
T <sub>panel,4</sub>	46.0146	0.4220	0.300	<b>0.5178 °C</b>
T <sub>panel,5</sub>	42.4207	0.8181	0.300	<b>0.8713 °C</b>
I <sub>pyra</sub>	560.478	6.2324	1.111	<b>6.3307W/m<sup>2</sup></b>
S <sub>panel</sub>	1.7521	0.00103	0.001	<b>0.00143m<sup>2</sup></b>
I <sub>rr</sub> *	982.010	-----	-----	<b>57.0816W</b>
V <sub>mp</sub>	26.6865	0.4189	0.100	<b>0.4306 V</b>
I <sub>mp</sub>	7.1291	0.1785	0.200	<b>0.2681 A</b>
P <sub>m</sub> *	131.247 9	-----	-----	<b>6.0797 W</b>
η *	0.2076	-----	-----	<b>0.0168</b>

\* Note: Results calculated from the uncertainty propagation law.

Table 2. Uncertainty of the variables on panel A.

PANEL B				
Variable	Mean	Uncert. Class A	Uncert. Class B	Uncertainty
T <sub>panel,1</sub>	40,0389	0.5631	0.3	<b>0.6380 °C</b>
T <sub>panel,2</sub>	37.2556	0.7383	0.3	<b>0.7969 °C</b>
T <sub>panel,3</sub>	35.3573	0.7763	0.3	<b>0.8322 °C</b>
T <sub>panel,4</sub>	33.8190	0.4757	0.3	<b>0.5624 °C</b>
T <sub>panel,5</sub>	33.8397	0.5654	0.3	<b>0.6400 °C</b>
T <sub>air,e,1</sub>	29.8217	0.8232	0.150	<b>0.8367 °C</b>
T <sub>air,e,2</sub>	29.2886	0.8993	0.150	<b>0.9117 °C</b>
T <sub>air,s,1</sub>	30.1329	1.0635	0.150	<b>1.0740 °C</b>
T <sub>air,s,2</sub>	31.1338	1.1042	0.150	<b>1.1143 °C</b>
v <sub>air,1</sub>	2.1893	0.000	0.060	<b>0.060 m/s</b>
v <sub>air,2</sub>	1.1013	0.000	0.060	<b>0.060 m/s</b>
I <sub>pyra</sub>	535.829	109.289	1.111	<b>6.4919W/m<sup>2</sup></b>
S <sub>panel</sub>	1.7521	0.00102	0.001	<b>0.00143 m<sup>2</sup></b>
I <sub>rr</sub> *	938.799	-----	-----	<b>11.3169 W</b>
V <sub>mp</sub>	18.8423	0.3839	0.100	<b>0.3968 V</b>
I <sub>mp</sub>	6.9683	0.1561	0.200	<b>0.2537 A</b>
P <sub>m</sub> *	131.248	-----	-----	<b>2.6281 W</b>
η *	0.4122	-----	-----	<b>0.0018</b>

\* Note: Results calculated from the uncertainty propagation law.

Table 3. Uncertainty of the variables on panel B.

As it is expected, these first measures show that the performance of the panel depends on the temperature reached by the panel, and that the lower the temperature is the higher the performance is.

In the following section, the dependence between panel temperature and the cross section of the space at the back of the photovoltaic panel is shown. The influence of air velocity on the performance is also shown.

#### 6. Influence of temperature on the electrical variables for different sections

To study the negative influence of temperature, several experiments have been made. The panels used are those used in the greenhouse. These have

been provided by ApiaXXI, the company supporting this study.

The specifications of the panels are shown in the table 5.

Peak power ( $P_{max}$ )	260 W
Maximum power voltage ( $V_{mp}$ )	36,00 V
Maximum power current ( $I_{mp}$ )	7,23 A
Open circuit voltage ( $V_{oc}$ )	43,49 V
Short circuit current ( $I_{sc}$ )	7,79 A

Table 5. Specifications of the panels used.

There have been four trials to compare the behavior of panel A with panel B. The difference between them is that we have changed the thickness, "b", of the air duct in panel B.

A data logger allows us to collect electrical variables ( $I_{mp}, V_{mp}, V_{oc}, I_{sc}$ ) and thermodynamic variables (Panels temperatures, Air temperatures, air velocity, solar irradiance/ $m^2$ ). Once obtained, we can calculate the total solar irradiance, peak power and the performance of each panel using the following equations.

$$I_{rr} = I_{pyra} \cdot S_{panel} \begin{cases} I_{rr} = \text{Irradiance (W)} \\ I_{pyra} = \text{Pyranometer measure (W/m}^2) \\ S_{panel} = \text{Panel area (m}^2) \end{cases}$$

$$P_m = I_{mp} \cdot V_{mp} \begin{cases} P_m = \text{Maximum power (W)} \\ I_{mp} = \text{Current (m.p.) (A)} \\ V_{mp} = \text{Voltage (m.p.) (V)} \end{cases}$$

$$\eta = \frac{P_m}{I_{rr}} = \frac{I_{mp} \cdot V_{mp}}{I_{pyra} \cdot S_{panel}} \quad \eta = \text{Panel performance}$$

We have collected values of each variable from 8.00 am to 3.00 pm. Every hour we have been collecting 25 values of each variable to obtain an average value.

The results obtained are shown in Table 6 for section 1 ( $b=0,075m$ ), Table 7 for section 2( $b=0,105m$ ), Table 8 for section 3 ( $b=0,135m$ ), and Table 9 for section 4 ( $b=0,165m$ ).

Case 1 ( $b=0.075m$ )					
$T^a_{amb}$	$Irr_A$	$T^a_{panelA}$	$Irr_B$	$T^a_{panelB}$	$\Delta T^a_{air}$
14,54	145,63	14,74	134,745	13,54	0,291
22,26	692,95	26,93	485,93	32,96	1,631
25,18	722,95	30,56	697,65	38,27	1,538
26,77	799,69	31,85	796,30	38,56	0,345
26,75	801,73	30,87	840,94	40,55	1,316
26,72	845,01	32,05	843,44	39,68	1,091
26,71	918,85	30,14	920,89	38,52	0,102
26,82	992,87	31,85	992,12	41,22	0,636

Table 6. Measured variables for case 1 during one day, from 8,00 until 15,00.

Case 2 ( $b=0.105m$ )					
$T^a_{amb}$	$Irr_A$	$T^a_{panelA}$	$Irr_B$	$T^a_{panelB}$	$\Delta T^a_{air}$
14,33	38,39	14,07	52,39	13,04	0,0435
18,24	328,41	19,71	314,30	32,17	0,673
24,14	332,70	27,53	433,46	24,56	0,100
20,85	667,52	24,46	676,41	32,71	0,567
23,43	669,92	26,77	685,76	34,05	0,232
22,925	836,93	28,10	814,11	41,68	0,875
26,45	858,28	32,35	861,51	37,72	0,729
25,07	971,05	32,48	966,67	41,07	0,082

Table 7. Measured variables for case 2 during one day, from 8,00 until 15,00.

Case 3 ( $b=0.135m$ )					
$T^a_{amb}$	$Irr_A$	$T^a_{panelA}$	$Irr_B$	$T^a_{panelB}$	$\Delta T^a_{air}$
10,16	47,11	10,02	49,19	9,08	0,320
14,49	350,76	18,01	362,40	19,48	1,392
21,04	530,00	37,35	530,00	34,82	1,258
25,74	607,94	37,28	602,78	35,80	0,944
24,14	607,99	32,14	668,23	36,69	1,205
24,03	656,48	33,45	751,30	43,21	1,826
26,29	736,09	37,78	808,49	41,978	0,955
25,60	864,94	38,45	868,03	44,07	2,128

Table 8. Measured variables for case 3 during one day, from 8,00 until 15,00.

Case 4 ( $b=0.165m$ )					
$T^a_{amb}$	$Irr_A$	$T^a_{panelA}$	$Irr_B$	$T^a_{panelB}$	$\Delta T^a_{air}$
11,75	54,01	11,31	57,51	10,10	0,101
16,77	309,41	22,13	314,77	34,05	1,452
25,82	319,99	32,02	317,02	34,27	0,938
26,01	348,24	32,53	353,60	32,84	1,036
22,59	571,38	35,35	578,39	37,39	3,451
29,07	717,72	40,29	706,65	45,09	3,205
27,76	745,67	44,82	748,88	48,53	5,157
30,79	810,93	46,88	783,51	52,45	4,599

Table 9. Measured variables for case 4 during one day, from 8,00 until 15,00.

For case 1( $b=0,075m$ ) and case 2 ( $b=0.105m$ ), with small thickness of the air duct. For irradiances values between 700-900 W, the panel B is 7-8 ° C warmer. (Fig.3 and Fig.4). However in case 3 ( $b=0.135m$ ) and case 4( $b=0.165m$ ) where the air duct has a greater thickness, the difference of the panels temperatures is 5 ° C (Fig.5 and Fig.6). For irradiances lower than 700W, in case 3 and 4 we can see in Fig.5 and 6 that both panels are more or less at the same temperature and in case 1 and 2 the panel B is 5-10°C hotter.

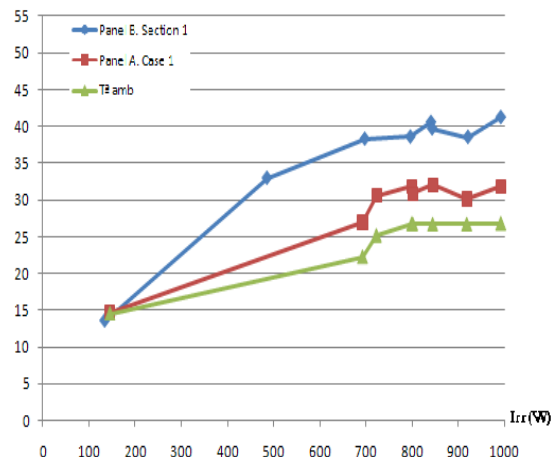


Fig. 3. Temperatures of the panels in case 1, with an air duct thickness  $b=0,075m$ .

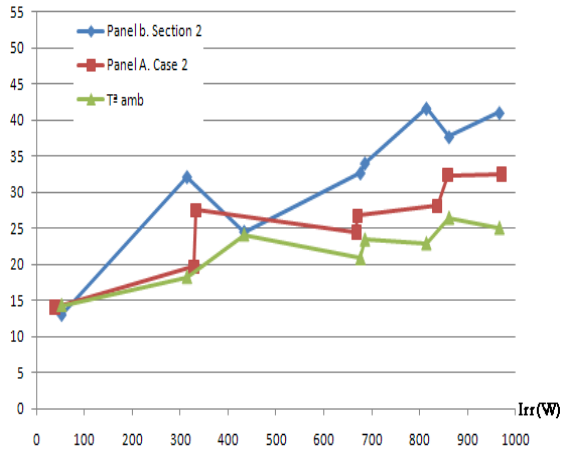


Fig. 4. Temperatures of the panels in case 2, with an air duct thickness  $b=0,105m$ .

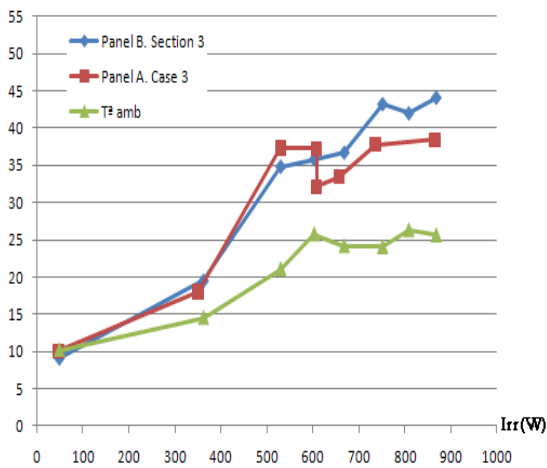


Fig. 5. Temperatures of the panels in case 3, with an air duct thickness  $b=0,135m$ .

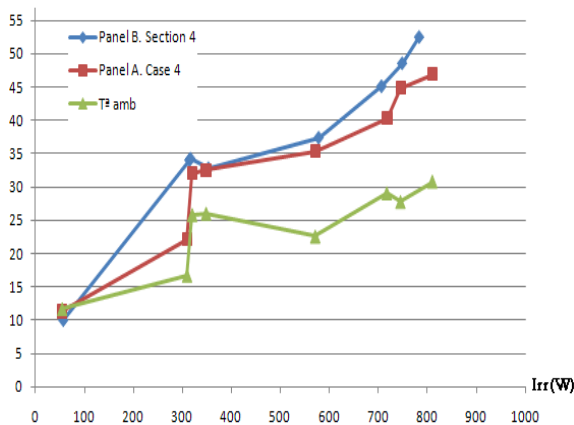


Fig. 6. Temperatures of the panels in case 3, with an air duct thickness  $b=0,165m$ .

In the Tables shown above (Table6-Table9) the measured values of the change in air temperature between the outlet and inlet duct have been included. As it is expected, the air at the outlet is warmer than the air at the inlet as the inlet temperature (ambient temperature) is a much lower

temperature than the panel temperature. Thus, there is a heat transfer between the panel and the air.

Figure 7 shows the changes in air temperature in different cases. At high irradiances (700-1000W), the changes in air temperature increase when the thickness "b" is greater, Section 3 and Section 4. This indicates that the air absorbs more heat from the panel and there is greater heat transfer. This Figure shows that a greater section of the air duct, panel B is cooled better and that the panel temperature will be lower, therefore the panel efficiency will not drop much.

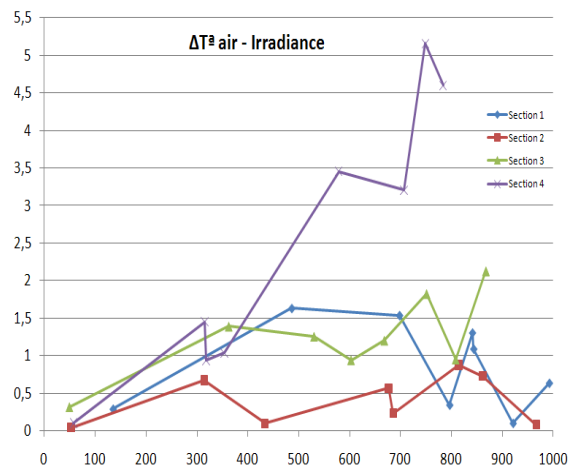


Fig.7. Variations of the air temperature in different cases.

As mentioned above, the temperature has a negative effect on the panel performance. Figure 8 shows that the maximum power voltage decreases with the increase of the panel temperature. Figure 9 instead shows that the maximum power current increases with the panel temperature. The decrease of the maximum power voltage is less than the increased of maximum power current, hence the peak power increase slightly with the panel temperature (Fig.10).

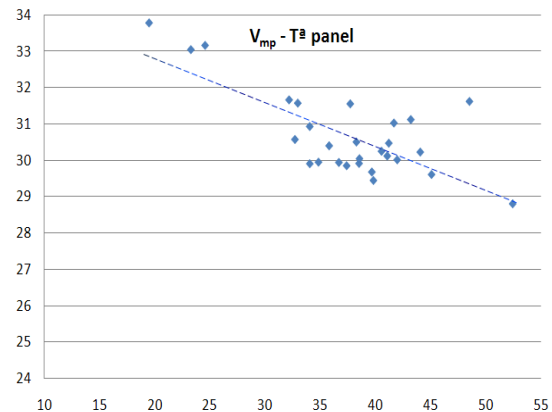


Fig.8. Maximum power voltage versus panel temperature.

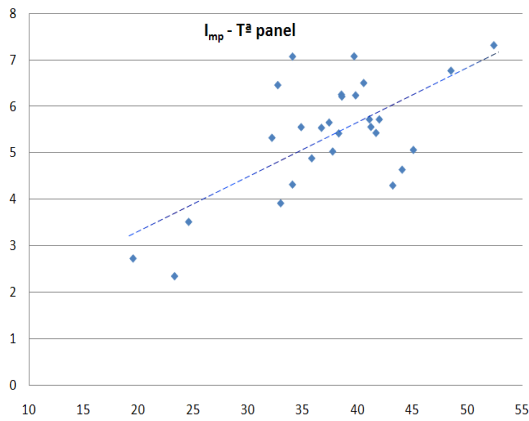


Fig.9. Maximum power current versus panel temperature.

Figure 10 also shows the irradiance versus panel temperature. The increase of the irradiance is much greater than the increase peak power, so the performance panel ( $\eta = \frac{P_m}{Irr}$ ) decreases considerably at high temperatures.

As explained before, in cases 1 and case 2 with small thickness ( $b$ ), the heat transferred between the panel and air is lower than cases 3, and 4, the panel will be hotter and its performance will be lower. This is illustrated in Figure 11. For panel temperatures above 35°C, the panel performance in cases 3 ( $b=0.135m$ ) and case 4 ( $b=0.165m$ ) is greater than case 1 ( $b=0.075m$ ) and case 2 ( $b=0.105m$ ).

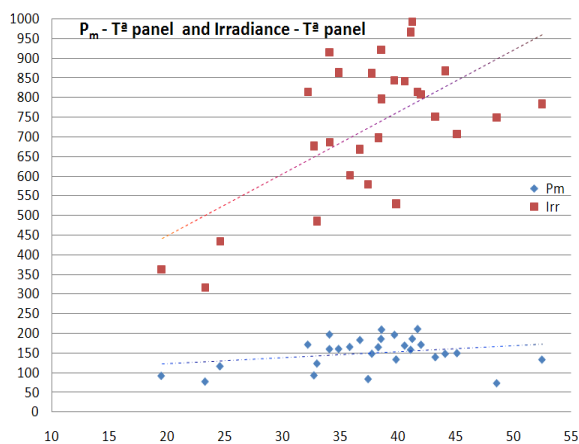


Fig.10. Peak power and irradiance versus panel temperature.

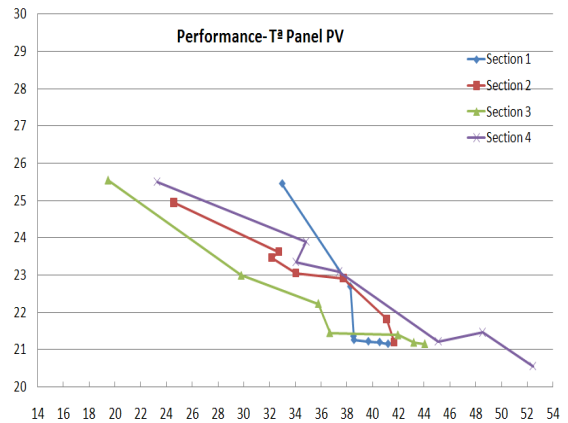


Fig.10. Performance of the panel B in different cases.

## 7. Conclusion

This abstract describes briefly, the installation built at the Technical University of Cartagena to study different methods to reduce the temperature of the photovoltaic panels and improve their efficiency. This is carried out by cooling the panels with air.

The study of the uncertainty analysis of all variables involved shows that uncertainties are very low and indicates that the measures taken and those calculated are reliable.

The results obtained for four different channels have been shown along this work. They advise that the space between photovoltaic panels and the greenhouse roof must be high enough to allow the panel to be refrigerated.

## REFERENCES

- [1] Angrist S. Direct energy conversion. Boston: Allyn and Bacon; 1982.
- [2] Hu C, White R. Solar cells: from basic to advance systems. New York: McGraw-Hill; 1983.
- [3] Graff K, Fischer H. Carrier lifetime in silicon and its impact on solar cell characteristics. In: Seraphin BO, editor. Topics in applied physics – solar energy
- [4] Arvind Tiwari, M.S. Sodha, Avinash Chandra, J.C. Joshi. Performance evaluation of photovoltaic thermal solar air collector for composite climate of India. Solar Energy Materials & Solar Cells 2006; 90: 175–189.
- [5] Guidelines for evaluating and expressing the uncertainty of NIST measurement results. NIST Technical note 1297, 1994 Edition.